Micromagnetic simulations of vortex-state excitations in soft magnetic nanostructures

F. Boust
Onera, 29 Avenue de la Division Leclerc, 92320 Châtillon, France

N. Vukadinovic*
Dassault Aviation, 92552 St-Cloud, France

(Received 30 April 2004; revised manuscript received 10 September 2004; published 17 November 2004)

The dynamic susceptibility spectra of Permalloy nanodots, supporting a vortex-type magnetic configuration, are studied within the frequency range 0.2–20 GHz as a function of dot thickness ($10\ \text{nm} \leqslant L_z \leqslant 80\ \text{nm}$) by means of three-dimensional dynamic micromagnetic simulations. In addition to the low-frequency vortex translation mode (gyrotropic motion of the vortex core), a second vortex core mode is revealed at a higher frequency for thicker nanodots (in-plane pumping field). This mode whose resonance frequency decreases rapidly with increasing dot thickness originates from the nonuniform vortex structure along the dot normal axis. Higher frequency modes are also observed for both in-plane and perpendicular pumping field orientations and correspond mostly to spin excitations localized outside the vortex core. The possible detection of the two vortex core modes within an individual nanodot using resonance experiments is discussed on the basis of the dispersion relation frequency versus perpendicular static magnetic field.

DOI: 10.1103/PhysRevB.70.172408 PACS number(s): 75.40.Gb, 75.40.Mg, 75.75.+a, 76.50.+g

The magnetic properties of nanoscale objects such as circular nanodots are today under great consideration mainly due to their potential applications in high-density magnetic storage and spin electronic devices.[1] It has been clearly stated that the equilibrium magnetic configuration within a soft ferromagnetic circular nanodot, depends on the nature of the magnetic material (mainly through the saturation magnetization M_s and the exchange constant A) and on geometrical properties, the dot radius R and the dot thickness L_z. A rich variety of nonuniform micromagnetic states (vortex, onion, in-plane buckling, etc.) was reported and their respective stability area was delimited within a phase diagram in the plane (thickness, radius).[2,3] Among these nonuniform configurations, the vortexlike structure appears in dots satisfying $L_z > \Lambda$ and $R \gg \Lambda$, where $\Lambda = \sqrt{2A/(\mu_0 M_s^2)}$ is the exchange length.[4,5] Such a vortex structure can be viewed as a curling in-plane magnetic configuration with a central region, the vortex core, in which the magnetization is tilted out of the dot plane [Fig. 1(a)]. The vortexlike magnetic configuration and several details of the vortex core region were evidenced by various experimental methods.[5–9]

In addition to these studies focused on the static magnetic configuration, the small-amplitude vortex state magnetic excitations are the subject of an increasing scientific interest during the past few years. Great efforts have been devoted to the development of analytical models[10–12] in order to analyze the magnetic excitation spectrum. A low-frequency vortex translation mode[10–12] and higher frequency spin wave modes[12] have been predicted assuming the invariance of the vortex magnetic configuration along the dot normal (limit of flat nanodots $L_z \ll \Lambda$). On the other hand, several preliminary numerical simulations of vortex state resonance modes have recently been reported.[13,14]

The purpose of this paper is to investigate the high-frequency linear magnetic excitations existing in a vortex magnetic configuration using dynamic micromagnetic simulations. The emphasis is placed on the effect of dot thickness on the dynamic susceptibility spectra. In addition, the role played by a polarizing magnetic field applied along the dot normal on the magnetic excitation spectra is also investigated.

The dynamic susceptibility spectra were determined using two three-dimensional (3D) codes developed by the authors.[15,16] The first one calculates a stable configuration of the magnetization vector by solving the Landau-Lifshitz equation in the time domain. The second one computes the full dynamic susceptibility tensor $\overline{\chi}$ ($\delta\mathbf{m} = \overline{\chi}\delta\mathbf{h}$, where $\delta\mathbf{m}$ is the dynamic magnetization response to a weak rf magnetic field $\delta\mathbf{h}$) from the linearization of the Landau-Lifshitz equation around the equilibrium configuration. The used material parameters are typical for isotropic Permalloy, namely, $M_s = 8.10^5$ A/m, $A = 1.3\ 10^{-11}$ J/m, and the gyromagnetic ratio $\gamma = 1.76\ 10^{11}\ \text{s}^{-1}\ \text{T}^{-1}$. The damping parameter corresponds to $\alpha = 0.025$. The dot radius value is fixed at $R = 80$ nm to keep reasonable computation time. The mesh sizes are $\Delta_x = \Delta_y = \Delta_z = 2.5$ nm.

Figure 1(b) represents the x component of the zero-field static magnetization M_x in the (x,y) plane for nanodots with $L_z = 20$ and 80 nm and for different z positions. The spiral spin arrangement is observed in which M_x varies continuously from negative values (blue color) to positive ones (red color) as we turn around the dot center. For the thinnest nanodot, the maps of M_x are nearly identical between the lower and upper dot surfaces. As the dot thickness increases, a twist appears between the two opposite surfaces. Such a deformation was previously reported[3] for the case of the onion state structure and arises from the search for the best flux closure between the end surface magnetic charges. It is worth noting that the vortex core radius depends significantly of the z coordinate with the smallest values at the dot surfaces (bottle-neck effect[3]). Furthermore, a sizeable radial component of the magnetization exists at the dot surfaces for the thickest nanodots.

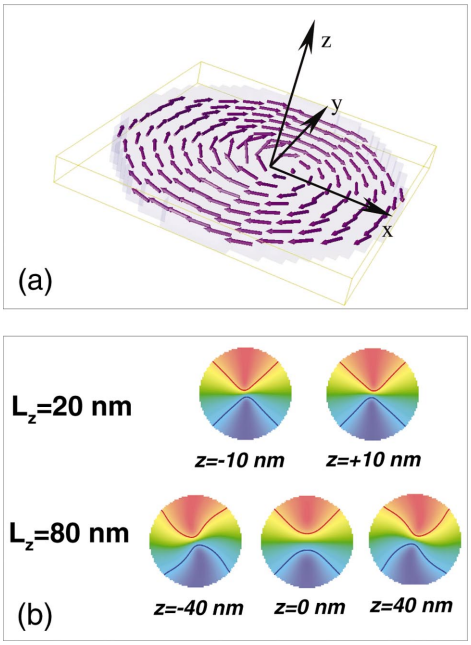

FIG. 1. (Color) 3D static micromagnetic simulations of nanodots with radius $R=80$ nm supporting a vortex magnetic structure at the remanent state. (a) Representation of the vortexlike structure and coordinate system. (b) M_x maps for the two thicknesses $L_z=20$ nm and $L_z=80$ nm. The color maps correspond to views in the plane (x,y) at different z positions (high level in red and low level in blue).

Figure 2 shows the imaginary part of the computed zero-field susceptibility spectra, in-plane element χ''_{xx},[25] within the frequency range 0.2-20 GHz. For the nanodot with thickness $L_z=20$ nm [Fig. 2(a)], three magnetic excitations, labeled (1), (2), and (3), respectively, are observed. The spatial distribution of resonance modes (color insets) indicates that the low-frequency resonance peak (resonance frequency $f_r=0.94$ GHz) arises from the spins localized within the vortex core. The resonance line (2) ($f_r=10.15$ GHz) results from spin regions with high values of M_y or M_z (excluding the peripheral zone of nanodots) whereas the resonance line (3) ($f_r=12.18$ GHz) is due to the excitation of spin areas with high values of M_y outside the vortex core.

For a thicker nanodot ($L_z=80$ nm), a new magnetic excitation, labeled (1′), appears ($f_r=3.55$ GHz). The spatial distribution of the resonance modes shows that the resonance lines (1) and (1′) correspond to vortex core spin excitations. For both modes, a twisted dynamic structure develops between the upper and lower dot surfaces. These modes appear nonuniform along the z axis, the resonance mode (1′) being strongly confined near the dot surfaces. The thickness dependence of resonance frequencies for the four resonance lines is displayed in Fig. 2(c). For the resonance line (1), the resonance frequency increases with dot thickness for $L_z<50$ nm, and then passes through a maximum before decreasing. This evolution is compared with the one deduced from the analytical model of Guslienko.[11] This model computes the resonance frequency of the low-frequency vortex translation mode corresponding to the precession movement of the vortex core around the dot center in the limit of flat nanodots.

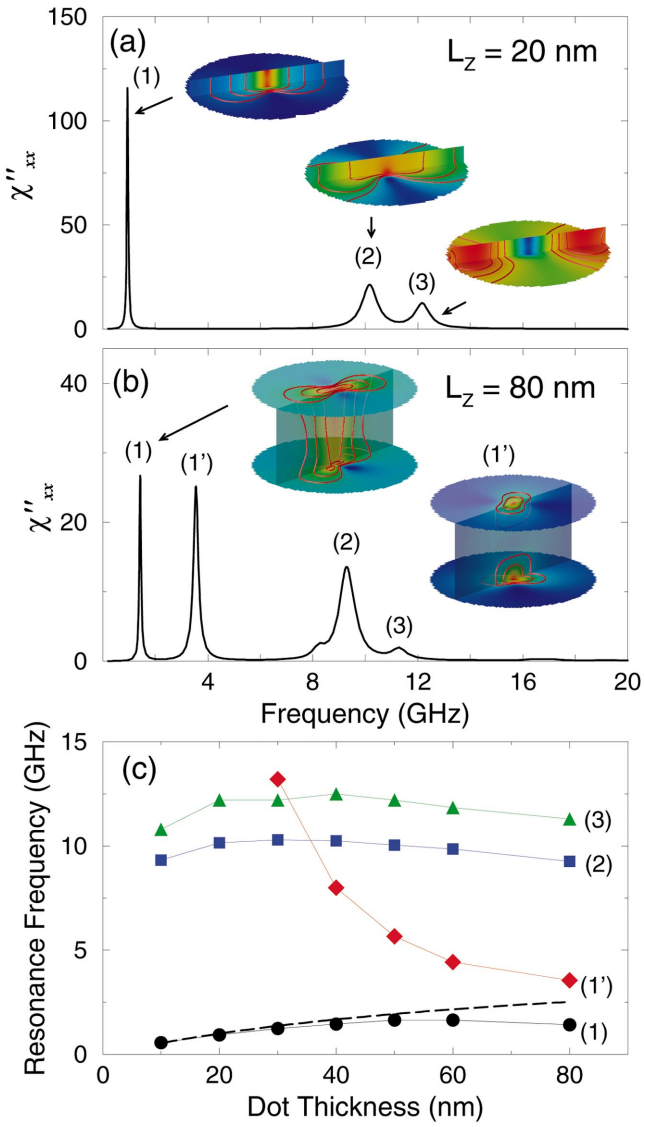

FIG. 2. (Color) 3D dynamic micromagnetic simulations of the nanodots defined in Fig. 1. Zero-field susceptibility spectra (imaginary part χ''_{xx}) for two dot thicknesses $L_z=20$ nm (a) and $L_z=80$ nm (b). The spatial distribution of resonant modes within the nanodots is displayed in the color insets (high level in red and low level in blue). (c) Thickness dependence of resonance frequencies for the four main modes. The dashed line corresponds to the Guslienko's model (Ref. 11).

The demagnetizing contribution includes only the volume magnetic charges and not the side magnetic charges usually considered in the rigid vortex model (translation of the rigid core without deformation).[10] This model reproduces the thickness evolution of the resonance frequency computed by the dynamic micromagnetic simulations very well for $L_z\leqslant 50$ nm. The resonance line (1′) depends strongly on dot thickness. This behavior is similar to the one of flexural domain wall modes existing in perpendicular magnetic thin films[17,18] and is related in both cases to the z dependence of magnetic static structure. The resonance frequencies of modes (2) and (3) vary weakly with dot thickness.

The zero-field spectra of χ''_{zz} (perpendicular element of the

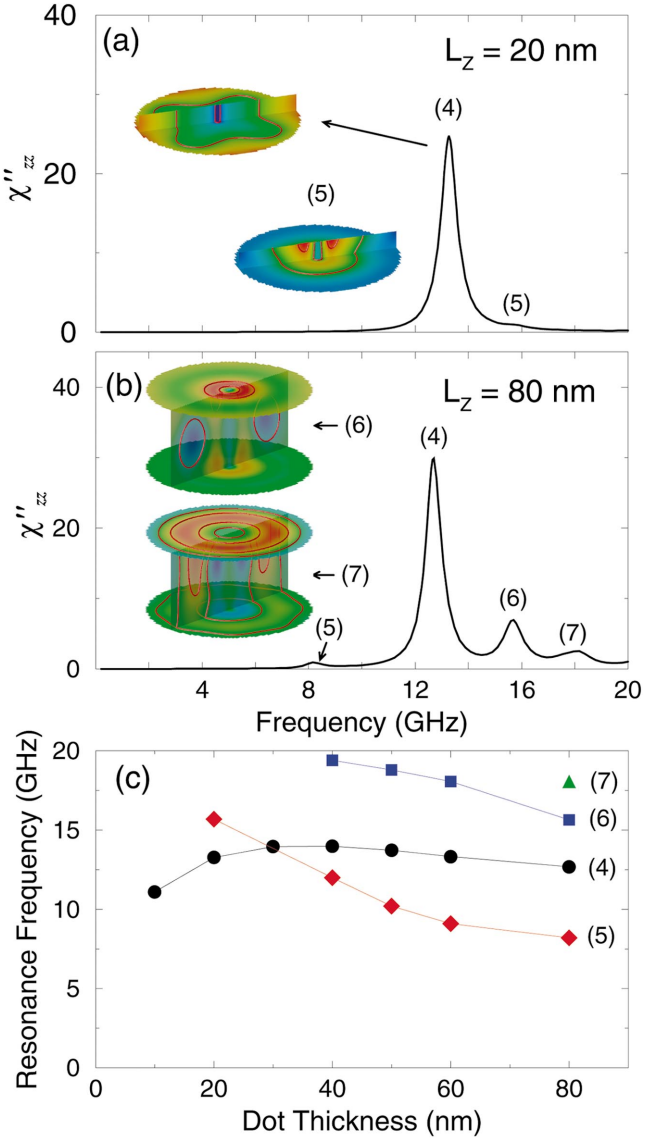

FIG. 3. (Color) 3D dynamic micromagnetic simulations of the nanodots defined in Fig. 1. Zero-field susceptibility spectra (imaginary part χ''_{zz}) for two dot thicknesses $L_z=20$ nm (a) and $L_z=80$ nm (b). (c) Thickness dependence of resonance frequencies for the three main modes. The conventions are the same as in Fig. 2.

dynamic susceptibility tensor) for the nanodots with $L_z=20$ nm and $L_z=80$ nm are displayed in Figs. 3(a) and 3(b), respectively. By comparison to the spectrum of χ''_{xx}, no magnetic excitations are observed below 8 GHz whatever the dot thickness is. The maps of modes confirm that no vortex core excitations are detected for this pumping field orientation due to the large values of M_z within the vortex core. For $L_z=20$ nm [Fig. 3(a)], the predominant resonance line (4) ($f_r=13.27$ GHz) is ascribed to the peripheral spin zone of the nanodot. The subsidiary resonance line (5) at a higher frequency ($f_r=15.7$ GHz) corresponds to a mode localized within a transition zone surrounding the vortex core. For $L_z=80$ nm [Fig. 3(b)], two additional magnetic excitations appear in the high-frequency side of the spectrum [resonance line (6) $f_r=15.65$ GHz and resonance line (7) $f_r=18.06$ GHz]. These modes are confined within a volume delimited by two concentric cylinders of the z axis. They are mainly distinguished by the radius of the cylinders which are greater for the mode (7) than for the mode (6). The thickness evolution of the resonance frequency for each resonance line is reported in Fig. 3(c). Within the investigated frequency and thickness ranges, the resonance frequencies of lines (5) and (6) decrease with increasing dot thickness whereas the one of the line (4) is an increasing function of L_z for small thicknesses ($L_z<40$ nm). The thickness dependence of the resonance frequency for the line (4) can be compared qualitatively with the one deduced from the analytical model reported in Ref. 19. This model allows the computation of eigenfrequencies of magnetostatic-type modes (dynamic exchange contribution is neglected) existing in a flat nanodot. In the limit of an edge-localized mode, this model leads to the lowest-order resonance frequency $f_r=8.6$ GHz for $L_z/R=0.15$, which is consistent with our numerical results ($f_r=11.3$ GHz). A better agreement would need the introduction of a more realistic mode profile [see Fig. 3(a)] in the analytical model.

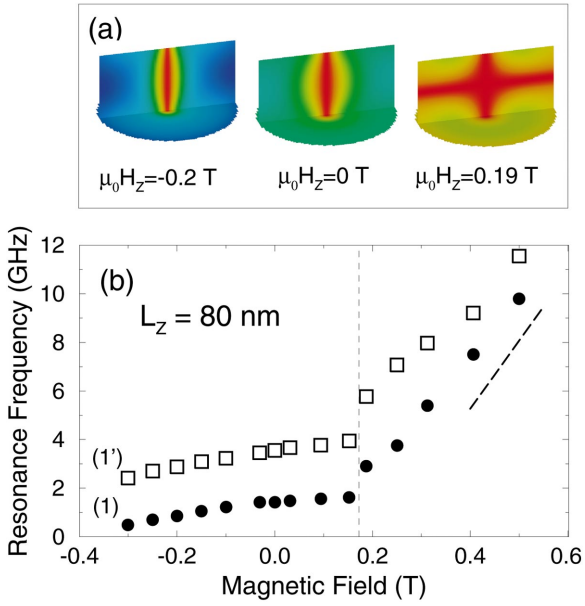

FIG. 4. (Color) Computed static and dynamic properties of the vortex core in the presence of a static magnetic field applied along the dot normal (z axis). The dot radius is $R=80$ nm and the dot thickness is $L_z=80$ nm. (a) Cross-sectional view (vertical plane through the dot center) of M_z. (b) Magnetic field evolution of the resonance frequencies for the two vortex core modes (symbols). The dashed line correspond to Kittel's law for an uniformly perpendicular magnetized dot.

Let us consider the effect of a polarizing magnetic field applied along the z axis (decreasing magnetic field values from $\mu_0H_z=0.5$ T down to $\mu_0H_z=-0.3$ T) for a nanodot with $L_z=80$ nm. Figure 4(a) shows the M_z component in a vertical plane crossing the dot center for different magnetic field values. For $\mu_0H_z<\mu_0H_{z,c1}=0.19$ T, a vortex configuration is stabilized. A diminution of the magnetic field value leads to a progressive decrease of the vortex core radius down to the vortex core switching, occuring at $\mu_0H_{z,s}=-0.37$ T.

The magnetic field evolution of the resonance frequencies for the two-lowest resonance lines is plotted in Fig. 4(b). Two regimes are clearly observed. For $H_{z,s} < H_z < H_{z,c1}$, the resonance frequencies of modes (1) and (1′) increase slowly with increasing magnetic field. The frequency gap between the two resonance frequencies is nearly constant. For $H_z \geqslant H_{z,c1}$, the slopes of the curves, resonance frequency versus magnetic field, are markedly steeper. Lastly, for $\mu_0 H_z > 0.5$ T (saturated regime), only the mode (1′) subsists. Its frequency-field dispersion curve approaches the one for the uniform gyromagnetic mode predicted by Kittel's law $\omega/\gamma = \mu_0[H_z - (1-3N_t)M_s]$, where $N_t \simeq 0.2627$ is the transverse demagnetizing factor.[20]

In summary, the vortex state excitations existing in magnetic nanodots, have been investigated using 3D dynamic micromagnetic simulations. For an in-plane pumping field, three (thin dot) or four (thick dot) magnetic resonance lines are observed within the frequency range 0.2–20 GHz. For the thick nanodots, the two-lowest resonance lines are attributed to vortex core modes. The second one at a higher frequency originates from the twisted static vortex structure and behaves similar to a flexural translation mode in perpendicular magnetization thin films. These results can provide a guide for experimentally evidencing such modes. A first observation of the lowest-frequency vortex core mode on an individual micron-scale dot was recently reported[21] using the time-resolved Kerr microscopy. It would be of great interest to extend this work and to try to detect, in particular, the second vortex core mode. Due to the wide frequency and magnetic field ranges where the vortex core modes exist, high-frequency resonance methods such as magnetic-resonance force microscopy (MRFM),[22] microwave microantenna technique,[23] or the use of a dc superconducting quantum interference device[24] could provide alternative methods to detect such excitations.

The authors thank S. Labbé for his help on numerical problems, B. Barbara for stimulating discussions, and the Délégation Générale pour l'Armement (DGA) of the French Defense Ministry which has supported the development of the micromagnetic codes.

*Email address: nicolas.vukadinovic@dassault-aviation.fr

[1] R. P. Cowburn, J. Magn. Magn. Mater. **242–247**, 511 (2002).
[2] K. L. Metlov and K. Y. Guslienko, J. Magn. Magn. Mater. **242–245**, 1015 (2002).
[3] J. K. Ha, R. Hertel, and J. Kirschner, Phys. Rev. B **67**, 224432 (2003).
[4] N. A. Usov and S. E. Peschany, J. Magn. Magn. Mater. **118**, L290 (1993).
[5] R. P. Cowburn, D. K. Koltsov, A. O. Adeyeye, M. E. Welland, and D. M. Trickner, Phys. Rev. Lett. **83**, 1042 (1999).
[6] M. Schneider, H. Hoffmann, and J. Zweck, Appl. Phys. Lett. **77**, 2909 (2000).
[7] J. Raabe, R. Pulwey, R. Sattler, T. Schweinbock, J. Zweck, and D. Weiss, J. Appl. Phys. **88**, 4437 (2000).
[8] T. Shinjo, T. Okuno, R. Hassdorf, K. Shigito, and T. Ono, Science **289**, 930 (2000).
[9] A. Wachowiak, J. Wiebe, M. Bode, O. Pietzsch, M. Morgenstern, and R. Wiesendanger, Science **298**, 577 (2002).
[10] N. A. Usov and L. G. Kurkina, J. Magn. Magn. Mater. **242–245**, 1005 (2002).
[11] K. Y. Guslienko, B. A. Ivanov, V. Novosad, Y. Otani, H. Shinia, and K. Fukamichi, J. Appl. Phys. **91**, 8037 (2002).
[12] B. A. Ivanov and C. E. Zaspel, Appl. Phys. Lett. **81**, 1261 (2002).
[13] R. Hertel and J. Kirschner, J. Magn. Magn. Mater. **272–276**, 655 (2004).
[14] F. Boust, N. Vukadinovic, and S. Labbé, J. Magn. Magn. Mater. **272–276**, 708 (2004).
[15] S. Labbé and P. Leca, C. R. Acad. Sci., Ser. I: Math. **327**, 415 (1998).
[16] S. Labbé and P. Y. Bertin, J. Magn. Magn. Mater. **206**, 93 (1999).
[17] J. C. Slonczewski, J. Magn. Magn. Mater. **23**, 305 (1981).
[18] N. Vukadinovic, J. Ben Youssef, and M. Labrune, Phys. Rev. B **66**, 132418 (2002).
[19] V. Novosad, M. Grimsditch, K. Y. Guslienko, P. Vavassori, Y. Otani, and S. D. Bader, Phys. Rev. B **66**, 052407 (2002).
[20] D.-X. Chen, J. A. Brug, and R. B. Goldfarb, IEEE Trans. Magn. **27**, 3601 (1991).
[21] J. Park, P. Eames, D. M. Engebretson, J. Berezovsky, and P. A. Crowell, Phys. Rev. B **67**, 020403 (2003).
[22] V. Charbois, V. V. Naletov, J. Ben Youssef, and O. Klein, J. Appl. Phys. **91**, 7337 (2002).
[23] M. Bailleul, D. Olligs, and C. Fermon, Phys. Rev. Lett. **91**, 137204 (2003).
[24] C. Thirion, W. Wernsdorfer, and D. Mailly, Nat. Mater. **2**, 524 (2003).
[25] The diagonal elements of $\overline{\chi}$ are unchanged when reversing the magnetization direction of the vortex core (polarization) or the rotational direction of the magnetization in the dot plane (vorticity).